Magnesium Technology 2011
Edited by: Wim H. Sillekens, Sean R. Agnew, Neale R. Neelameggham, and Suveen N. Mathaudhu
TMS (The Minerals, Metals & Materials Society), 2011

STUDY ON THE GRAIN REFINEMENT BEHAVIOR OF Mg-Zr MASTER ALLOY AND Zr CONTAINING COMPOUNDS IN Mg-10Gd-3Y MAGNESIUM ALLOY

Guohua Wu[1, 2], Ming Sun[1, 2], Jichun Dai[1, 2], Wenjiang Ding[1, 2]
[1]National Engineering Research Center of Light Alloy Net Forming; Shanghai Jiaotong University; Shanghai, 200240, China
[2]State Key Laboratory of Metal Matrix Composites; Shanghai Jiaotong University; Shanghai, 200240, China

Keywords: Grain refinement, Magnesium alloy, Zirconium (Zr)

Abstract

The effects of Mg-Zr master alloy and a potassium fluozirconate (K_2ZrF_6) salt mixture (KSM) on the grain refinement behavior of Mg-10Gd-3Y magnesium alloy were studied. The results show that the Mg-10Gd-3Y alloy is well refined by Mg-Zr or KSM. The characteristic microstructure feature of the alloy refined by Mg-Zr master alloy is the Zr-rich cores that exist in most grains, while the Zr-rich cores are not observed in the alloy refined by KSM. It is suggested that the grain refinement mechanisms of zirconium in the two cases are different: the Zr released from Mg-Zr master alloy works by adding heterogeneous nucleants, while the Zr produced from the in-situ reaction between Mg melt and K_2ZrF_6 works by restricting grain growth. Compared with the Mg-30.wt%Zr master alloy, the KSM refiner shows much longer fading time during melting.

Introduction

The recently developed Mg-Gd-Y-Zr alloys are becoming one of the most promising heat-treatable magnesium alloys, because they exhibit excellent specific strength at both room and elevated temperatures, and its creep resistance is markedly better than that of WE54, which until now has been the most creep resistant commercially available magnesium alloy [1-4].

In Mg-RE alloys, the powerful grain refiner, Zr, leads to a fine and equiaxed microstructure, which is needed for structural uniformity and consistency in performance of Mg-products [5]. Hitherto, many papers have studied the grain refinement behavior of adding Zr into magnesium alloys [6-16]. Over the decades various approaches to introducing Zr into molten magnesium alloy have been explored, including alloying with different forms of Zr metal, alloying with Zr sponge, alloying with Zn-Zr, with ZrO_2, with Zr-salts, or with Mg-Zr master alloys [10, 16]. Although, in principle, zirconium may be introduced into magnesium by a number of approaches, it appears that only Mg-Zr type master alloys have been in widespread use since 1960 because of the disadvantages of other alloying approaches [10, 11, 15]. However, during the alloy casting process, the utilization rate of Mg-Zr master alloy is not satisfactory (low alloying efficiency [8]) because the undissolved Zr particles spontaneously settle due to the much higher density of Zr (~6.52 g/cm^3) than liquid Mg (~1.7 g/cm^3) [12], and that large zirconium particles (>5μm) are inactive as nucleation centers [6]. Consequently, an excess of Mg-Zr master alloy needs to be introduced in order to achieve the satisfactory zirconium content for optimum grain refinement, which greatly increases the cost [8]. Therefore, work reconsiders the relatively cheap, convenient and easily handled Zr-salt method, and experiments related to the grain refinement effect of K_2ZrF_6 on magnesium alloy have been performed and reported in our recent paper [17].

Moreover, most of the published papers concerning the grain refinement effect of Zr on magnesium alloys only focus on alloying with Mg-Zr master alloy, which may not be too comprehensive for understanding the precise mechanism by which Zr works. The grain refinement mechanism of Zr is still the subject of investigation. So, this study also furthers the knowledge of the grain refinement by Zr addition into magnesium.

Experimental Procedures

The Mg-10Gd-3Y-0.5Zr (GW103K) alloy was prepared from high purity Mg (99.95wt.%) and master alloys of Mg-25wt.%Gd and Mg-25wt.%Y in an electric resistance furnace under a mixed flowing protective gas of CO_2 and SF_6 with the volume ratio of 100:1. Two forms of Zr grain refiner including Mg-Zr master alloy (microstructure as shown in Figure 2) and a potassium fluozirconate (K_2ZrF_6) salt mixture (KSM, composition of 50wt.%K_2ZrF_6-25wt.%NaCl-25wt.%KCl) were used respectively to compare their grain refinement behaviors. For the former, the addition order was Mg→Mg-25%Gd→Mg-25%Y→Mg-30%Zr. However, for the latter, the addition order was Mg→Mg-25%Gd→KSM→Mg-25%Y, where KSM is added before melting Mg-Y because Y can preferentially react with the K_2ZrF_6 causing loss of Y. After the designed holding time, it was cast at 750 °C into metallic molds preheated to 150 °C.

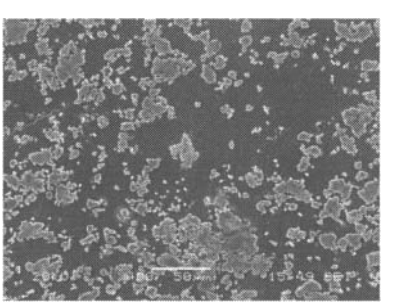

Figure 1. SEM microstructure of as-received Mg-30wt.%Zr master alloy.

A combination of optical microscopy (OM, OLYMPUS BX51M), scanning electron microscopy (SEM, JEOL JSM-6460), electron probe micro-analyzer (EPMA, JXA-8800R), transmission electron microscope (TEM, JEOL 2010), energy dispersive X-ray spectrometry (EDS, Oxford INCA) was carried out to characterize as-cast microstructure. Specimens for microstructure observation were etched in a 4 vol.% nital solution.

Results and Discussion

Grain Refinement Efficiency

The connection between average grain size (AGS) and Zr content is shown in Figure 2 [17, 18]. It can be seen that the AGS reduces with an increase of Zr content regardless of the difference in the two refiners. The AGS of alloy with 0.93% Zr refined by Mg-Zr master alloy is the finest (22μm), while the alloy with 0.56% Zr refined by KSM is the finest (21μm). Hence, it is possible that the grain refinement efficiency of in-situ Zr chemically reduced from the K_2ZrF_6 salts is much better than that of the ex-situ Zr released from the Mg-Zr master alloy.

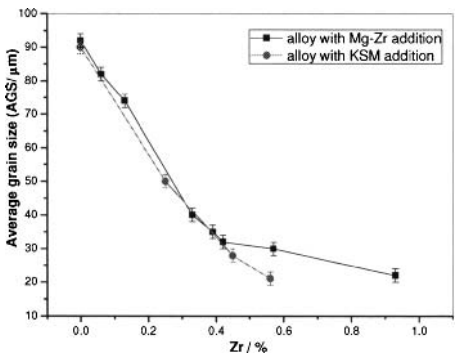

Figure 2. Relationship between Zr content and average grain size (AGS) of Mg-10Gd-3Y-Zr alloys.

Microstructures

Figures 3 and 4 show the microstructures of the alloy refined by Mg-Zr master alloy and the alloy refined by KSM, respectively. They all consist of primary α-Mg matrix and the β-$Mg_{24}(Gd, Y)_5$ eutectic phase distributed along the grain boundaries [17, 18].

The microstructures of alloys with different Zr contents, which are refined by Mg-Zr, are shown in Fig. 3. It can be seen that the AGS reduces with an increasing Zr content. Because the solubility of Zr in molten magnesium at the peritectic temperature (653.6°C) is only ~0.445% and increases to ~0.6% at 780 °C [13], and there are no intermetallics in Mg-Zr binary phase diagram, some undissolved Zr particles are present in the alloy with 0.93% Zr content. Previous report showed that magnesium melts inoculated with Zr particles always contain some undissolved Zr particles even though the addition of Zr is below the solubility limit [13]. Therefore, Figure 3 (c) shows that undissolved Zr particles may also caused grain refinement effect. This is in good agreement with Ma's study [13] which shows that nucleation of magnesium grains occurred on two types of zirconium nucleants, where the first type were formed by precipitation, and the other type were undissolved particles. The conclusion is further testified by Figure 3 (d) which shows that a sample with 3.67%Zr taken from the bottom of the melt has very fine grain size (10μm). Moreover, it is recently shown by Tamura et al. that undissolved Zr particles actually play an important role in grain refinement [19], and more recent work [12, 13, 20] has confirmed this observation and demonstrated that grain refinement of magnesium alloys by Zr is dictated by both soluble and insoluble Zr contents.

An obvious distinction between the Zr-rich cores (the halo structures formed in the melt, which are Zr-rich magnesium crystallites [13]) in Figure 3 (b) and Figure 3 (c) is that the former is petal-like while the latter is spherical. Ma [13] indicates that the major factor noticed affecting the growth patterns of Zr-rich halo is the dissolved Zr content: the magnesium halo structures in a low Zr content magnesium melt is much more prone to dendritic growth than those formed in a high Zr content magnesium melt.

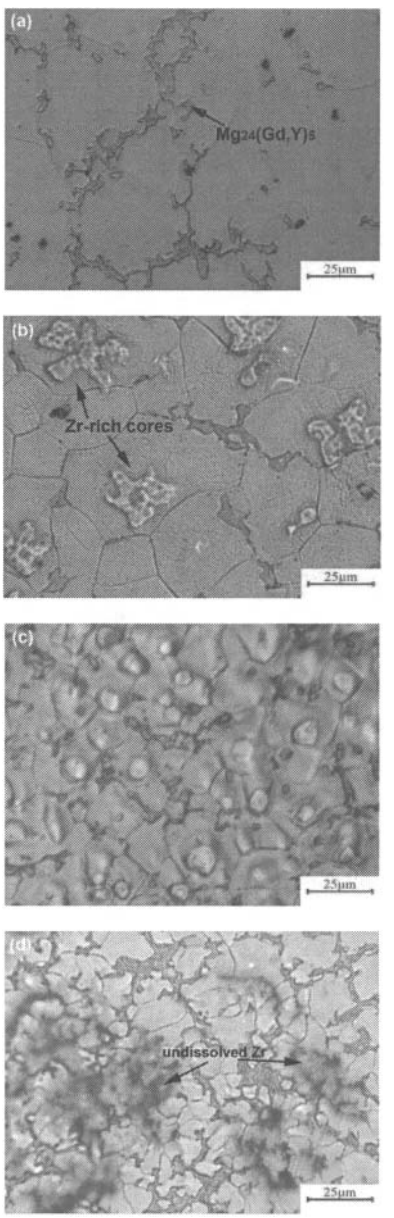

Figure 3. Optical microstructures of as-cast alloys with different Zr contents (wt.%), (a) 0; (b) 0.42; (c) 0.93, and (d) 3.67%, a sludge sample taken from the bottom of the melt has very fine grain size (~10μm).

Figure 4 shows the influence of KSM addition level on the microstructure of GW103 alloy. It is clear that with increasing addition level from 0% to 12% (wt.%), the AGS of GW103K alloy decreases gradually. However, the addition of the salt mixture causes inclusions whose compositions are composed of fluorides, chlorides and oxides which result from the chemical reduction reaction: $K_2ZrF_6+2Mg=Zr+2MgF_2+2KF$. Our previous paper [17] has clarified that the reason for the presence of inclusions whose compositions are mainly O, F, Cl, Na, K, Mg, Gd, Y and Zr is possibly that the reaction products of KF and MgF_2 combined with the residual KSM to form inclusion clusters.

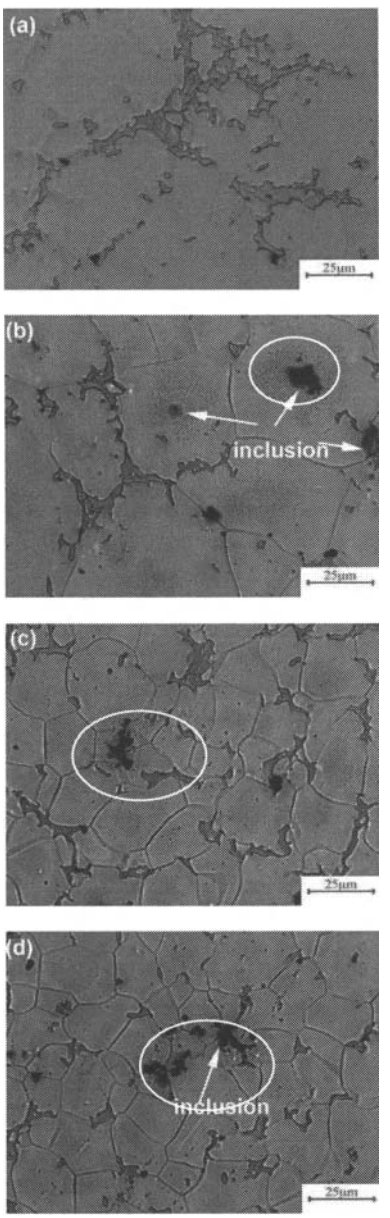

Figure 4. Microstructure of GW103K alloy with different KSM addition level: (a) 0, (b) 4%, (c) 8%, (d) 12%.

Different Existing Feature of Zr

Although both of the two agents can well refine the Mg-10Gd-3Y alloys, the presence of Zr in the alloys is different. As shown in Figure 3, the Zr-rich cores or undissolved Zr particles are obvious in the alloys refined by Mg-Zr master alloy, similar to the previous literatures [1, 9, 17]. The characteristic Zr-rich cores in Figure 5 illustrate that some small white Zr particles located at the centre of the Zr-rich cores which then form Zr clusters and act as nucleates.

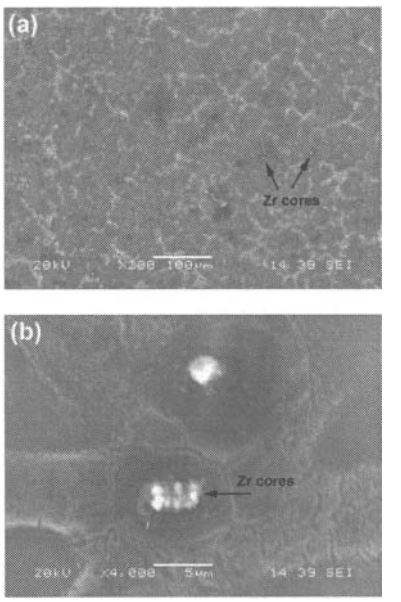

Figure 5. SEM morphology of the Zr cores in the model alloy Mg-10-Gd-3Y-0.52Zr alloy at: (a) low magnification and (b) high magnification.

Figure 6 shows TEM images and corresponding EDS results of the particles in the alloy refined by Mg-Zr, further indicating that Zr is meant as α-Zr, which is in good agreement with previous observations [1, 10].

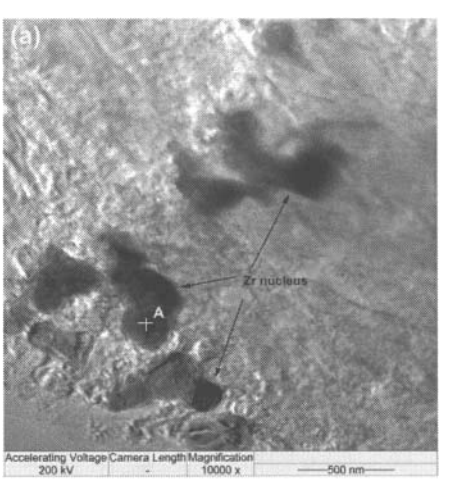

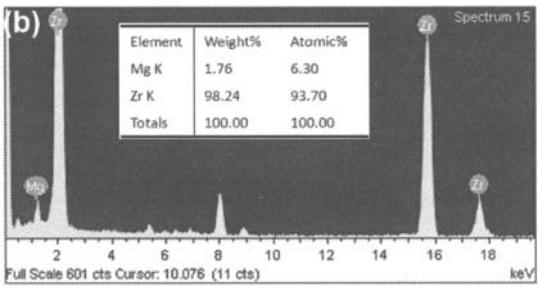

Figure 6. (a) TEM image, (b) EDS of Zr nucleus.

However, the Zr-rich cores are not observed in the alloy refined by K_2ZrF_6 as shown in Fig. 3, and the Zr element distribution is uniform detected by EPMA scanning as shown in Figure 7. So it is possible to believe that the in-situ tiny Zr well dissolves into the magnesium melt and then causes the grain refinement effect.

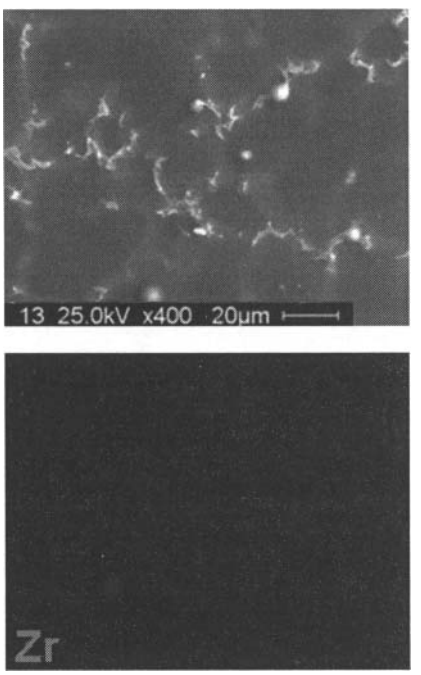

Figure 7. EPMA surface distribution of the element Zr in the 8% KSM processed sample.

Discussion

Although the microstructural feature of Zr distribution in the two alloys is different, the grains are both well refined. The mechanism by which Zr works may be different. For the alloy refined by Mg-Zr, the grain refinement mechanism may be explained by the most popular peritectic mechanism proposed by Emley [21]: since α-Zr and α-Mg have the same crystal structure (*hcp*) and nearly same lattice parameters (Zr: a_{Zr}=0.323nm, c_{Zr}=0.514nm; Mg: a_{Mg}=0.320nm, c_{Mg}=0.520nm), suitably sized α-Zr particles may act as effective nucleant sites for magnesium. The most characteristic feature of the microstructure of a magnesium alloy containing more than a few tenths per cent soluble Zr is the Zr-rich cores that exist in most grains [7]. They are believed to be the products of peritectic solidification. However, for the alloy refined by K_2ZrF_6, where the in-situ Zr dissolves well in the Mg matrix, the grain refinement mechanism can be understood from a growth restriction perspective. According to Lee's calculations [22], the solute Zr has the strongest growth restriction factor (GRF) among the common alloying elements in Mg, such as Ca, Si, Zn, Cu, Al, Sc, Sr, Ce, Y, etc, which makes Zr have powerful grain refinement effect on Mg. Here, the GRF theory means that the solute elements generate constitutional undercooling in a diffusion layer ahead of the advancing solid/liquid interface and then restrict grain growth [22-24]. Consequently, for the alloy refined by K_2ZrF_6, the growth restriction effect of Zr is well established, in which the K_2ZrF_6 salts approach introduced into magnesium alloy produces a large number of in situ fresh Zr particles, and then the dissolved Zr facilitates the grain refinement from a growth restriction perspective. Similarly, Peng [23] finds that, in the Mg-9Gd-4Y-Zr alloys, there is at least one zirconium rich core in almost each grain in alloys with high zirconium content, whereas the characteristic zirconium rich cores are not found in the alloy with low zirconium content. He suggests that the grain refinement mechanism of zirconium in the low zirconium alloy is different from that in the high zirconium alloys: the zirconium works mainly by generating nucleants in the high zirconium alloys, and by restricting grain growth in the low zirconium alloy.

The fading time of the two studied grain refiners is compared in Figure 8. It can be seen that by extending the holding time to 120 min, the Zr content in the alloy refined by KSM almost keeps stable. However, the Zr content in the alloy refined by Mg-30wt.%Zr master alloy gradually fades with increasing holding time. In particular, it decreases significantly after 120 min, indicating that the grain refinement effect of the Mg-Zr master alloy only lasts for a short time after addition [25]. Therefore, the K_2ZrF_6 salt mixture refiner has a much longer fading time comparing that of Mg-Zr master alloy. This is similar with previous study on refining effect of salts containing Ti and B elements in purity aluminum compared with that of an Al-Ti-B master alloy [26].

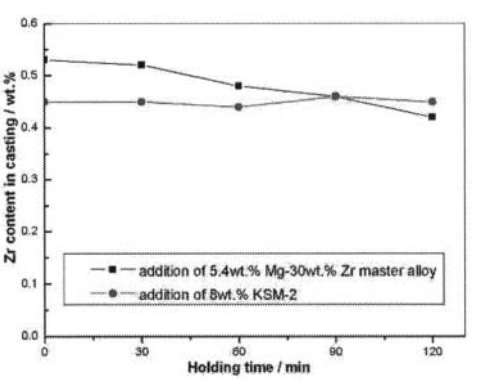

Figure 8. Comparison of the fading time of grain refinement between the addition of 8wt.% KSM and that of 5.4wt.% Mg-30wt.%Zr master alloy. Industrially the latter can yield 0.4~0.6wt.% Zr content in magnesium alloys.

Furthermore, because the total Zr content detected by ICP-AES in the alloy refined by KSM consists of well dissolved Zr content and the inclusion's Zr content, it is reasonable to deduce that, a relatively lower dissolved Zr content may be enough for a satisfactory grain refinement effect. In other words, if the Zr recovery of KSM could be improved by technical methods, the KSM approach has more potential. Based on the above analysis, further work of melting and purification will be investigated to improve the K_2ZrF_6 approach in order to increase the Zr recovery and to remove the subsequent inclusions.

Conclusions

The Mg-10Gd-3Y alloy is grain refined by a Mg-Zr master alloy and KSM. The characteristic microstructural feature of the alloy refined by the Mg-Zr master alloy is Zr-rich cores that exist in most grains, while the Zr-rich cores are not observed in the alloy refined by KSM. It is suggested that the grain refinement mechanisms of zirconium in the two cases are different: the Zr released from Mg-Zr master alloy works by adding heterogeneous nucleation, while the Zr reduced from the in-situ reaction between the Mg melt and K_2ZrF_6 works by restricting grain growth. Compared with the Mg-30.wt%Zr master alloy, the KSM refiner shows much longer fading time during melting.

Acknowledgements

The present study is funded by the National Basic Research Program of China (No. 2007CB613701), Program of Shanghai Subject Chief Scientist (No. 08XD14020) and Aerospace Science and Technology Innovation Fund of China Aerospace Science and Technology Corporation (No. 0502).

References

1. S.M. He, X.Q. Zeng, L.M. Peng, X. Gao, J.F. Nie, W.J. Ding, "Microstructure and Strengthening Mechanism of High Strength Mg-10Gd-2Y-0.5Zr Alloy," *J. Alloys Compd,.* 427 (2007), 316-323.
2. Y.C. Guo, J.P. Li, J.S. Li, Z. Y, J. Zhao, F. Xia, M.X. Liang, "Mg-Gd-Y System Phase Diagram Calculation and Experimental Clarification," *J. Alloys Compd.,* 450 (2008), 446-451.
3. W. Wang, Y.Huang, G. Wu, Q. Wang, M. Sun, W. Ding, "Influence of Flux Containing YCl_3 Additions on Purifying Effectiveness and Properties of Mg-10Gd-3Y-0.5Zr Alloy," *J. Alloys Compd.,* 480 (2009), 386-391.
4. T. Honma, T. Ohkubo, S. Kamado, K. Hono, "Effect of Zn Additions on the Age-Hardening of Mg-2.0Gd-1.2Y-0.2Zr Alloys," *Acta Mater.,* 55 (2007), 4137-4150.
5. Ma Qian, Z.C.G. Hildebrand, D.H. StJohn, "The Loss of Dissolved Zirconium in Zirconium-Refined Magnesium Alloys after Remelting," *Metall. Mater. Trans. A,* 40A (2009), 2470-2479.
6. Ma Qian, D. StJohn, M.T. Frost, "Heterogeneous Nuclei Size in Magnesium-Zirconium Alloys," *Scripta Mater.,* 50 (2004), 1115-1119.
7. Ma Qian, D. StJohn, M.T. Frost, "Characteristic Zirconium-Rich Coring Structures in Mg-Zr Alloys," *Scripta Mater.,* 46 (2002), 649-654.
8. Ma Qian, A. Das, "Grain Refinement of Magnesium Alloys by Zirconium: Formation of Equiaxed Grains," *Scripta Mater.,* 54 (2006), 881-886.
9. P. Cao, Ma Qian, D.H. StJohn, M.T. Frost, "Uptake of Iron and its Effect on Grain Refinement of Pure Magnesium by Zirconium," *Mater. Sci. Technol.,* 20 (2004), 585-592.
10. Ma Qian, D. StJohn, M.T. Frost, "Zirconium Alloying and Grain Refinement of Magnesium Alloys," *Magnesium Technology 2003,* Ed. H. Kaplan, pp. 209-214, San Diego, USA: TMS.
11. Ma Qian, D. StJohn, M.T. Frost, M. R. Barnett, "Grain Refinement of Pure Magnesium Using Rolled Zirmax-Master Alloy (Mg-33.3Zr)," *Magnesium Technology 2003,* Ed. H. Kaplan, pp. 215-220, San Diego, USA: TMS.
12. Ma Qian, L. Zheng, D. Graham, M.T. Frost, D.H. StJohn, "Settling of Undissolved Zirconium Particles in Pure Magnesium Melts," *J. Light Met.,* 1 (2001), 157-165.
13. Ma Qian, D.H. StJohn, "Grain Nucleation and Formation in Mg-Zr Alloys," *International Journal of Cast Metals Research,* 22 (2009), 256-259.
14. Ma Qian, "Heterogeneous Nucleation on Potent Spherical Substrates during Solidification," *Acta Mater.,* 55 (2007), 943-953.
15. Ma Qian, D. Graham, L. Zheng, D. H. StJohn, M. T. Frost, "Alloying of Pure Magnesium with Mg-33.3wt%Zr Master Alloy," *Mater. Sci. Technol.,* 19 (2003), 156-162.
16. Ma Qian, D. StJohn, M.T. Frost, "Magnesium Zirconium Alloying," US Patent 0 161 121 A1, 2005.
17. M. Sun, G.H. Wu, J.C. Dai, W. Wang, W.J. Ding, "Grain Refinement Behavior of Potassium Fluozirconate (K_2zrf_6) Salts Mixture Introduced into Mg-10Gd-3Y Magnesium Alloy," *J. Alloys Compd.,* 494 (2010), 426-433.
18. M. Sun, G.H. Wu, W. Wang, W.J. Ding, "Effect of Zr on the Microstructure, Mechanical Properties and Corrosion Resistance of Mg-10Gd-3Y Magnesium Alloy," *Mater. Sci. Eng. A,* 523 (2009), 145-151.
19. Y. Tamura, N. Kono, T. Motegi, E. Sato, "Grain Refining Mechanism and Casting Structure of Mg-Zr Alloy," *Journal of Japan Institute of Light Metals,* 48 (1998), 185-189.
20. D.H. StJohn, A.K. Dahle, T. Abbott, M.D. Nave, Ma Qian, "Solidification of Cast Magnesium Alloys," *Magnesium Technology 2003,* Ed. H. Kaplan, pp. 95-100, San Diego, USA: TMS.
21. E. F. Emley, *Principles of Magnesium Technology* (Oxford: Pergamon Press, 1966), 257-261.
22. Y. C. Lee, A. K. Dahle, D. H. StJohn, "The role of solute in grain refinement of magnesium," *Metall. Mater. Trans. A,* 31A (2000), 2895-2906.
23. Z.K. Peng, X.M. Zhang, J.M. Chen, Y. Xiao, H. Jiang, "Grain Refining Mechanism in Mg-9Gd-4Y Alloys by Zirconium," *Mater. Sci. Technol.,* 21 (2005), 722-726.
24. D.H. StJohn, Ma Qian, M. Easton, P. Cao, Z. Hildebrand, "Grain Refinement of Magnesium Alloys," *Metall. Mater. Trans. A,* 36A (2005), 1669-1679.
25. H.E. Friedrich, and B.L. Mordike, *Magnesium Technology: Metallurgy, Design Data, Application* (Berlin Heidelberg: Springer-Verlag Berlin Heidelberg, 2006), 128-135.
26. H.H. Zhang, X. Tang, G.J. Shao, L.P. Xu, "Refining Mechanism of Salts Containing Ti And B Elements in Purity Aluminum," *J. Mater. Process. Technol.,* 180 (2006), 60-65.